ELSEVIER

Biochimica et Biophysica Acta 1505 (2001) 82–93

BIOCHIMICA ET BIOPHYSICA ACTA
BBA

www.bba-direct.com

Review

Na^+-driven flagellar motor of *Vibrio*

Tomohiro Yorimitsu, Michio Homma *

Division of Biological Science, Graduate School of Science, Nagoya University, Chikusa-ku, Nagoya 464-8602, Japan

Received 29 May 2000; received in revised form 18 October 2000; accepted 18 October 2000

Abstract

Bacterial flagellar motors are molecular machines powered by the electrochemical potential gradient of specific ions across the membrane. Bacteria move using rotating helical flagellar filaments. The flagellar motor is located at the base of the filament and is buried in the cytoplasmic membrane. Flagellar motors are classified into two types according to the coupling ion: namely the H^+-driven motor and the Na^+-driven motor. Analysis of the flagellar motor at the molecular level is far more advanced in the H^+-driven motor than in the Na^+-driven motor. Recently, the genes of the Na^+-driven motor have been cloned from a marine bacterium of *Vibrio* sp. and some of the motor proteins have been purified and characterized. In this review, we summarize recent studies of the Na^+-driven flagellar motor.

Keywords: Bacterial flagellar motor; Na^+-driven motor; Torque generation; Na^+ channel blocker; *Vibrio alginolyticus*

1. Introduction

Flagella are the rotary machines that convert the ion flux to the locomotive force of the cell. Bacteria have helical flagellar filaments extending from the cell body. They swim toward favored environments in liquid media by reversibly rotating the flagellar filaments, which function as propellers. Each flagellum is driven by a rotary motor embedded in the cytoplasmic membrane at its base. The flagellar basal part (the rotor) in Gram-negative bacteria is composed of more than 10 protein components, and consists of the rod and the four ring structures, termed L ring, P ring, MS ring, and C ring. It is speculated that the C ring is surrounded by stator particles (force-generating units) (Fig. 1) [1–4]. However, the C ring is not tightly bound to the basal part and is easily lost in a purification procedure (Fig. 1c). The rotation of the flagellar motor is powered by the electrochemical gradient of specific ions across the cytoplasmic membrane. In 1977, it was shown that the flagellar motors of *Bacillus subtilis* and *Streptococcus* spp. can be driven by an artificial H^+ gradient [5,6], indicating that the energy source of the motor is the proton-motive force. It has been shown that the motors of other bacteria, such as *Escherichia coli* and *Salmonella typhimurium*, are also energized by H^+ influx [3,7,8].

The force-generating units, which form the stator, are composed of two proteins, MotA and MotB [9,10]. MotA has four transmembrane segments and one large cytoplasmic loop [11]. MotB has a single N-terminal transmembrane segment and a peptidoglycan binding motif at the C-terminus [12–14]. These components form a complex to function as a H^+ channel [15–19]. It is inferred that their trans-

* Corresponding author. Fax: +81-52-789-3001;
E-mail: g44416a@nucc.cc.nagoya-u.ac.jp

0005-2728/01/$ – see front matter
PII: S0005-2728(00)00279-6

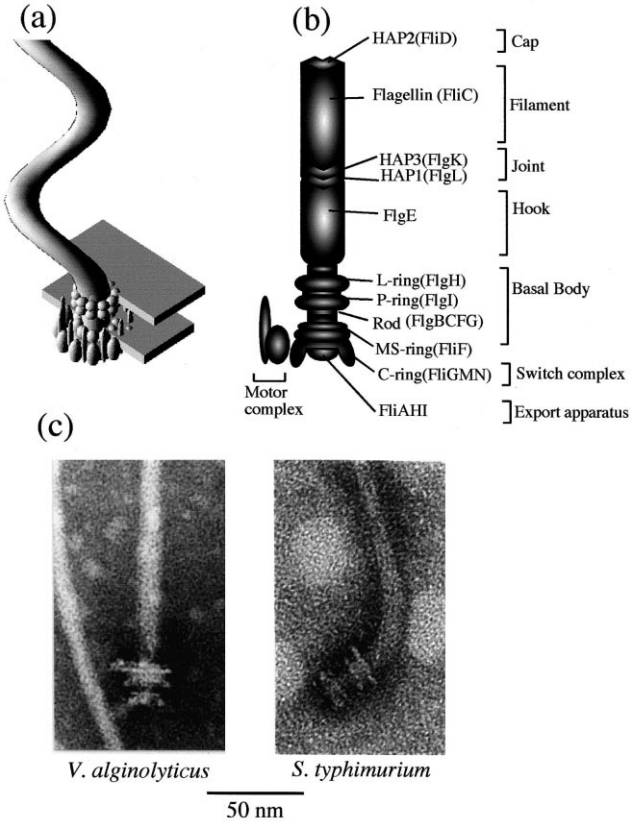

Fig. 1. Structure of flagella. (a) Cartoon of a flagellar structure of Gram-negative bacteria. (b) The components and substructure of flagella. (c) Electron micrographs of a filament–hook–basal body complex which is stained by phosphotungstate. The switch complex (C ring), motor complex, and export apparatus are missing.

membrane segments, which are predicted to form α-helices, make an ion channel. One of the most prominent hypothesis is that structural changes induced in MotA generate the rotary power by coupling H^+ flow to changes of the interaction with the rotor component FliG, as discussed later [20–24]. The mechanism of coupling between the H^+ flow and the structural changes has not been resolved.

In some bacteria, the flagellar motor is powered by the electrochemical gradient of Na^+ [25]. Early studies of the Na^+-driven flagellar motor were carried out using alkaliphilic *Bacillus*. Alkaliphilic *Bacillus* optimally lives and is vigorously motile at pH 10–11 [26]. Under alkaline conditions, the H^+-motive force is quite small because the intracellular pH of these bacteria is maintained at pH 8–9 by the mechanism of homeostasis [27]. It was shown that the presence of Na^+ in the medium was essential for the motility of these bacteria [28] and it was proved that the flagellar motor of these bacteria rotates by the electrochemical potential of Na^+ [29–31]. Some *Vibrio* spp., *V. alginolyticus*, *V. parahaemolyticus*, and *V. cholerae*, use the Na^+-motive force to rotate polar flagellar motors [32–36]. It is known that *V. alginolyticus* and *V. parahaemolyticus* also have H^+-driven lateral flagella [34,37] (Fig. 2a). These marine *Vibrio* species use the Na^+-driven polar flagella for swimming in liquids, such as sea water, and the H^+-driven lateral flagella for swarming in viscous environments, such as on surfaces of fish [38,39]. As shown in Fig. 2b, the swimming speed generated by the polar flagella decreases rapidly as the buffer viscosity is increased, and stops at a viscosity of 200 cP. In contrast, the swimming speed by the lateral flagella increases with viscosity to about 5 cP of viscosity, then decreases gradually, but is still about 20 μm/s at 200 cP viscosity [40]. *V. alginolyticus* as well as other *Vibrio* spp. have the Na^+-translocating respiratory chain and Na^+/H^+ antiporter, which extrude Na^+ and might generate the electrochemical potential for the Na^+-driven flagellar motor [41]. Thus wild-type Na^+ motility is resistant to the H^+ conductor CCCP, but the motility of mutant cells with a defective Na^+ pump is sensitive to CCCP (Fig. 2c) [42].

The Na^+-driven motor has advantages for the study of its function because the Na^+-motive force can be more easily manipulated, and the motor function can be inhibited by specific Na^+ channel blockers, which are also powerful tools for the study of the energy-coupling mechanism of the motor.

2. Components essential for the torque generation of the Na^+-driven motor

At first, the Na^+-driven flagellar motor was predicted to contain motor components homologous to MotA and MotB of the H^+-driven flagellar motor. Using homology, it was attempted to clone the genes from bacteria that have Na^+-driven flagella. However, the strategy was not successful. The Na^+-driven motor genes were cloned using motility-defective mutants. The essential genes, *motX* and *motY*, for the rotation of the Na^+-driven motor were identified and

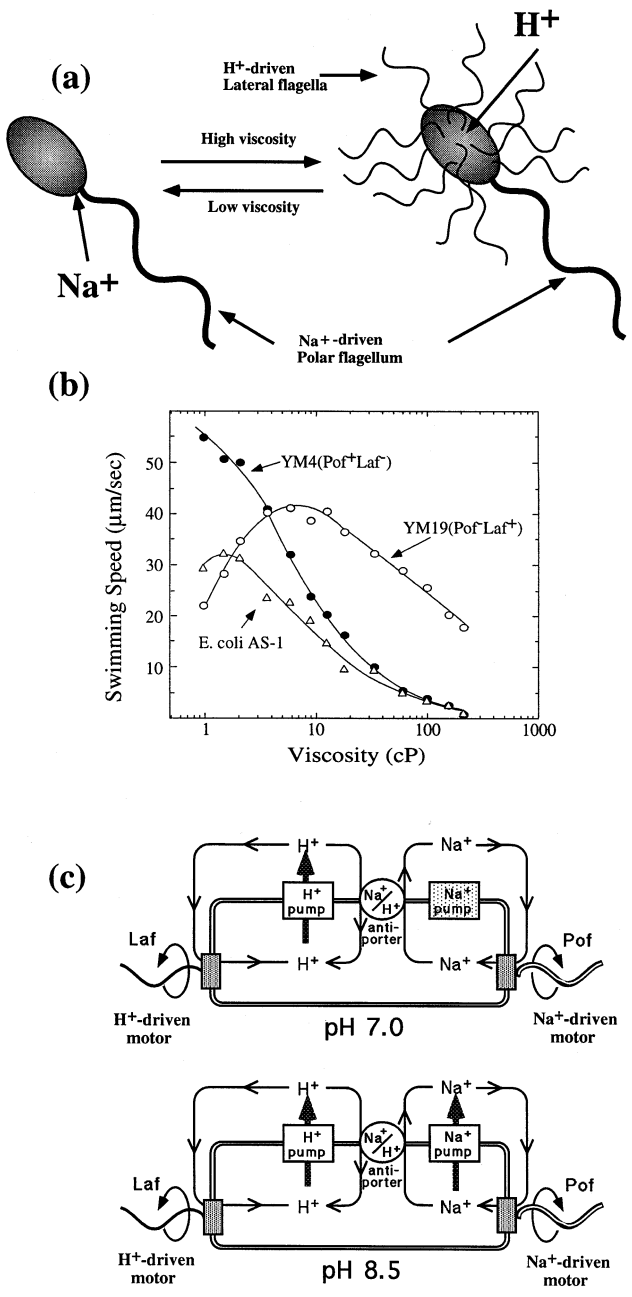

Fig. 2. Lateral flagella and polar flagellum of *V. alginolyticus*. (a) Differentiation of flagellar system of *V. alginolyticus*. (b) Functional difference between Laf and Pof with regard to viscosity [40]. The swimming speed was measured in a buffer in which the viscosity was changed by addition of polyvinylpyrrolidone. (c) Circulation of Na^+ and H^+ under the different pH conditions for the flagellar motors of *V. alginolyticus*. In *V. alginolyticus*, Na^+ and H^+ are pumped out by the respiratory chain and the Na^+ pumping is only active in the alkaline condition. The H^+ gradient can be changed to a Na^+ gradient by antiporters.

cloned from *V. parahaemolyticus* [43,44]. The *motX* and *motY* genes were also identified in *V. alginolyticus*, closely related to *V. parahaemolyticus* [45,46]. From the deduced amino acid sequences, it is assumed that these two components, MotX and MotY, are membrane proteins with a single transmembrane segment, and indeed both of them are separated in a membrane fraction. MotY has a peptidoglycan binding motif (which is also observed in MotB, an essential component of the H^+-driven motor) in its C-terminal region [13,14]. In the H^+-driven motor, it is suggested that the interaction with peptidoglycan and the motif is important for fixing the MotA/MotB complex around the rotor. On the other hand, MotX might form a part of the Na^+ channel because overexpression of MotX causes *E. coli* to be defective in growth when the extracellular Na^+ concentration is increased. The growth defect is rescued by amiloride [44], which is known to be a potent inhibitor of Na^+ channels as well as the Na^+-driven flagellar motor [47]. Moreover, MotY failed to be localized to the cytoplasmic membrane in the absence of MotX. MotA is required for the stability of MotB in *E. coli* cells [48]. From these lines of evidence it was speculated that MotX and MotY form a complex of force-generating unit similar to the complex of MotA and MotB. However, overall similarities with MotX and MotY were not found in the components of the H^+-driven motor. Therefore, it had been assumed that the mechanisms of the energy conversion with ion flux were very different between the H^+- and the Na^+-driven motors.

In 1997, two novel genes, *pomA* and *pomB*, which are essential for rotating the Na^+-driven flagellar motor in *V. alginolyticus*, were isolated [49]. The amino acid sequences of PomA and PomB are similar to those of MotA and MotB, respectively. By random mutagenesis of the *pomA* gene, it has been suggested that PomA and MotA are very similar in structure and function [50]. It is inferred that PomA has four transmembrane segments, and PomB has a single transmembrane segment and a peptidoglycan binding motif in the C-terminal region. PomA and PomB are most likely to interact with each other because they are co-precipitated with each other and the stability of PomB is dependent on the presence of PomA in the cell [51]. The complex of PomA and PomB seems to function as a Na^+ channel. Recently, homologous

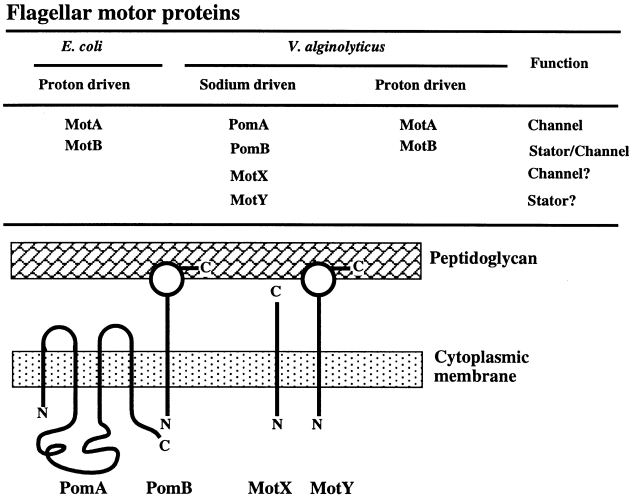

Fig. 3. Gene productions for the H^+-driven motor and the Na^+-driven motor. Membrane-localized components for the H^+-driven motor of *E. coli* and the Na^+-driven and H^+-driven motors of *V. alginolyticus* are summarized. The predicted membrane topology of the four motor gene products in the Na^+-driven motor is illustrated as previously [49].

genes were isolated in *V. parahaemolyticus* [52]. Further, four homologous genes are found also in the genome sequence of *V. cholerae*. These results suggest that the force-generating unit of the Na^+-driven flagellar motor is composed of four components, PomA, PomB, MotX, and MotY (Fig. 3).

3. Rotation analysis of the Na^+-driven flagellar motor

The rotation rate of the flagellar motor of *V. alginolyticus* was measured by laser dark-field microscopy. Laser dark-field microscopy is a powerful tool because it enables the measurement of the rotation speed of a single flagellar motor. In this method, a cell is stuck and fixed on the glass surface and its rotating flagellum is irradiated by a laser beam. The intensity of scattered light is detected by a photon-counting system, and then the rotation rate of a single flagellum is measured from the change of the intensity [53]. In *V. alginolyticus*, it was shown that the rotation rate of a flagellum was proportional to the speed of a freely swimming cell [54]. The swimming speeds and the flagellar rotation rates of individual free-swimming cells were measured simultaneously, and a roughly linear relation between swimming speed and flagellar rotation rate was observed [55]. In other words, the flagellar rotation rate can be estimated from the swimming speed. The average rotation rate of the flagellar motor is 1100 rps and the highest value is 1700 rps [56]. On the other hand, the rotation rates for the H^+-driven motor of *E. coli* and *S. typhimurium* were measured as ca. 300 rps [57] and ca. 200 rps [53], respectively. This remarkable difference of the rotational rates might reflect the difference of the efficiencies for the energy coupling between the H^+- and Na^+-driven motor. In Table 1, various motors including the ATP-driven motors are compared. Many possible mechanisms for ion-driven rotary motors have been proposed, although without reliable supporting evidence [58]. The Na^+-driven flagellar motor is inferred to be the fastest motor among those that we know [56]. The *Vibrio* Na^+-driven flagellar motor may be adapted to high-speed rotation.

4. Specific inhibitors of the Na^+-driven flagellar motor

The functions of mammalian Na^+ channels, Na^+/H^+ exchangers and Na^+/Ca^{2+} exchangers have been analyzed using amiloride, one of the specific inhibitors of Na^+-coupled systems [59]. Amiloride is

Table 1
Statistics for various motors

	Flagella of *E. coli*	Polar flagella of *V. alginolyticus*	F_1 motor of F_0F_1-ATPase	Myosin of skeletal muscle
Axis distance	ca. 20 nm	ca. 20 nm	ca. 1 nm	NA
Rotational speed	300 rps	1700 rps	10 rps	NA
Linear speed	40 μm/s	210 μm/s	60 nm/s	10 μm/s
Torque/generator	ca. 450 pN nm	ca. 100 pN nm	ca. 40 pN nm	NA
Force	ca. 25 pN	ca. 5 pN	ca. 40 pN	ca. 5–10 pN
Efficiency	~100% ??	~100% ??	~100% ??	~50% ??
Energy source	H^+	Na^+	ATP	ATP

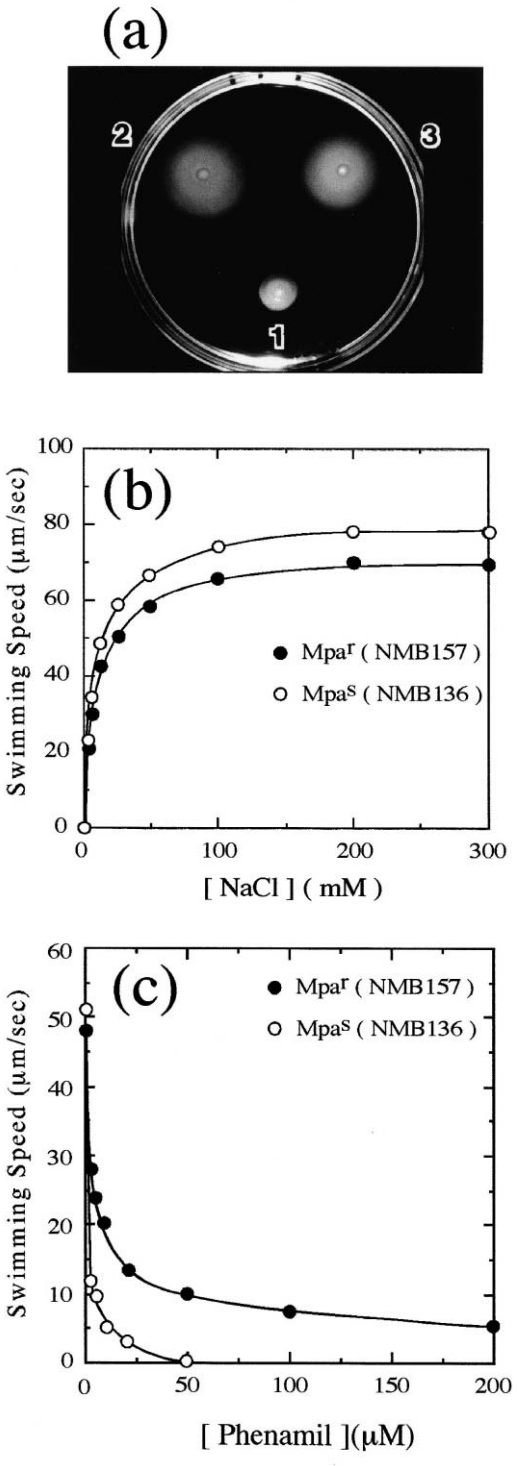

Fig. 4. Characterization of motility mutants resistant to phenamil. (a) Swarming abilities of the mutants in the presence of phenamil. 1, the Mpa^s (wild-type for the phenamil sensitivity) strain; 2 and 3, the Mpa^r mutants (motility mutants resistant to phenamil). (b) Relationship between Na^+ concentration of the medium and swimming speed was examined for the Mpa^s strain and the Mpa^r mutant. (c) Motility inhibition of the Mpa^s strain and the Mpa^r mutant by phenamil was examined. The data are quoted from [64].
←

thought to bind to the Na^+ binding site in the channel. It was found that amiloride also specifically inhibits the function of the Na^+-driven flagellar motor, without affecting the membrane potential, the intracellular pH homeostasis, or the ATP content of the cells and only slightly affecting the Na^+-coupled amino acid transport system in alkaliphilic *Bacillus* [47]. The inhibition of cell motility by amiloride is reduced with increasing Na^+ concentration in the medium. This result indicates that amiloride reversibly inhibits the motor function by competing with Na^+.

6-Iodoamioride (6-IA), which is a photoreactive amiloride analog, competitively and reversibly inhibits the rotation of the flagellar motor of alkaliphilic *Bacillus*. However, 6-IA irreversibly inhibits the motility after irradiation with UV light. When tethered cells of alkaliphilic *Bacillus* were irradiated with UV light in the presence of 6-IA, the rotation rate gradually decreased in five to nine steps, suggesting that there are multiple torque generators that function independently in the Na^+ motor [60]. Similar results have been obtained in the H^+-driven motor [61,62]. When MotB was inducibly produced in a tethered *motB* cell of *E. coli*, the rotation rate of the cell increased stepwise for a maximum of eight steps. Moreover, by electron microscopy, about 10 particles which might be the torque generators were found in the cytoplasmic membrane, and they are absent in motor-defective mutants [63]. From the electron microscopic images, the basal body structures of the H^+- and Na^+-driven flagella are similar to each other (Fig. 1c). These results suggest that the number of torque generators is around 10 in both the H^+- and Na^+-driven motors.

To study the Na^+ binding site of the Na^+-driven flagellar motor of *V. alginolyticus*, Kojima et al. [64] isolated motility mutants resistant to phenamil, an amiloride analog (Fig. 4a). The swimming speeds of both strains showed a similar dependence on the external Na^+ concentration (Fig. 4b). The wild-type cells for motility cannot swim at 50 μM of phenamil,

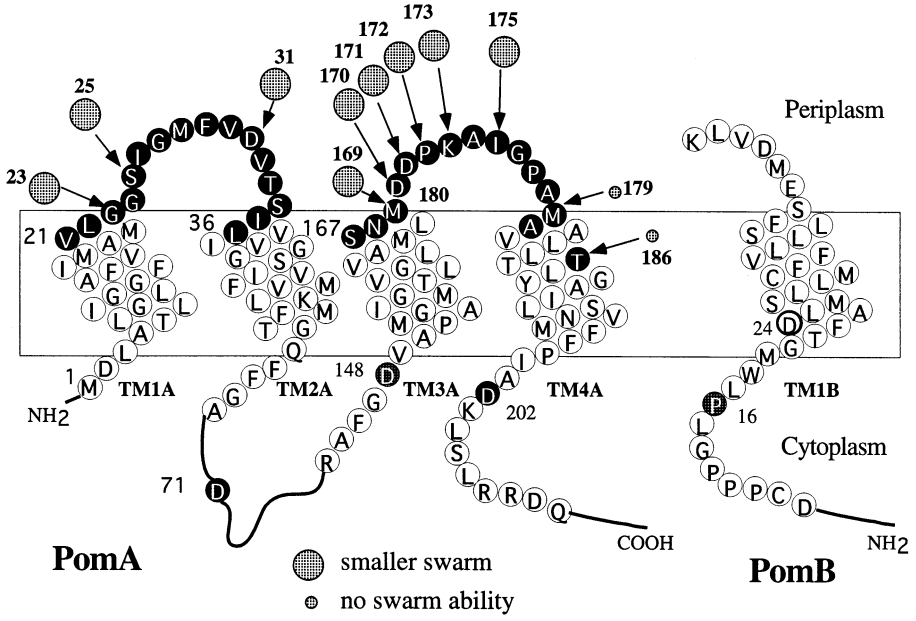

Fig. 5. Model of the membrane topology of PomA and PomB. Positions substituted by Cys are shown as closed circles with the white letters of amino acids [66]. Relative swarm sizes in the Cys mutants are indicated by the shaded circles. Where no shaded circle is given, swarm size was similar to that of the wild-type cells. The shaded circles with the white letters (D148 of PomA and P16 of PomB) show the mutation sites for the phenamil resistance. The thick circle (D24 of PomB) shows a possible Na^+ binding site.

while the mutant cells can swim at this concentration (Fig. 4c). Unlike amiloride, the effect of phenamil on the motor function is not dependent on the concentration of Na^+ in the medium. The fluctuation of the rotation rate of the motor, which is defined as the standard deviation divided by the average rotation rate, was investigated by laser dark-field microscopy. It was shown that the rotation rate of the wild-type flagella greatly fluctuates in the presence of phenamil, but that of the mutant resistant to phenamil does not. This work suggests that the motor has the phenamil-specific binding site and the resistant phenotype is explained by increasing the dissociation rate of phenamil to the motor. Phenamil is likely to bind near the Na^+ binding site. The mutations providing the phenamil-resistant motility are independently mapped in *pomA* and *pom*B genes, and consist of substitution of Asp^{148} to Tyr in PomA or Pro^{16} to Ser in PomB (Fig. 5) [65]. From the predicted topology of PomA and PomB, it is predicted that each residue is located near the cytoplasmic ends of transmembrane segments (Fig. 5). The double mutation of PomA-D148Y/PomB-P16S synergistically impairs motility in the absence of phenamil and makes the motility less sensitive to phenamil. Those lines of evidence suggest that Asp^{148} of PomA and Pro^{16} of PomB are proximally located, and that multiple residues of both PomA and PomB including Asp^{148} and Pro^{16}, respectively, contribute to the formation of the high-affinity phenamil binding site. Analysis of motor function by Na^+ channel inhibitors was also carried out to isolate amiloride- and phenamil-resistant mutants, and the mutation sites were characterized in *V. parahaemolyticus* [52]. In the PomA homolog in *V. parahaemolyticus*, mutations at the same position (Asp^{148}) provide the phenamil-resistant phenotype. Mutations at Gly^{20} and Ala^{23} and the deletion of Pro^{12} to Pro^{16} caused resistance to phenamil in the PomB homolog. Phenamil resistance mutation sites have been found only in PomA or PomB, not in any other components for torque generation. In both species, no amiloride-resistant mutations have been assigned. The high-affinity binding site for phenamil is likely to be composed of the multiple residues of PomA and PomB which form a Na^+ channel. The high-affinity site seems to be close to Asp^{24} of PomB which is the candidate of the Na^+ binding site (see below).

5. The role of the periplasmic loop regions of PomA

There are two putative periplasmic loops, $loop_{1-2}$ and $loop_{3-4}$, in PomA. The loops may help to maintain the arrangement of the membrane-spanning helices that form the ion channel, guide the Na^+ ion or interact with the ions, or with other proteins, such as PomB. By Cys-scanning analysis, the periplasmic loops of PomA were investigated for functional and topological information (Fig. 5) [66]. From profiles of labeling by biotin maleimide, the membrane topology of $loop_{3-4}$ was directly predicted, on the other hand, the residues of $loop_{1-2}$ were not labeled. This suggests that the environments of the two loops are very different. $Loop_{1-2}$ may be covered with a protein, such as PomB, MotX, or MotY, or may be embedded in the pore region of the channel. In $loop_{3-4}$, many Cys substitutions and the five successive mutations from M169 to K173 impaired motility, and only the M179C mutation abolished motility. From the evidence that the reactivity of D170C to SH-modifying reagents changed with the Na^+ concentration, it is speculated that D170 faces towards the channel pore and interacts with Na^+, or that Na^+ changes the structure around D170. The residues from M169 to K173 may not be essential but play an important role for the motor function.

When PomA with an introduced Cys residue (Cys-PomA) in the C-terminal periplasmic loop ($loop_{3-4}$) was examined without exposure to a reducing reagent, a 43-kDa band was observed in some mutants, whereas only a 25-kDa band, which corresponds to monomeric PomA, was observed under reducing conditions [67]. The 43-kDa band was strongest in the P172C mutant. The intensity of the 43-kDa band was enhanced in most mutants by the oxidizing reagent $CuCl_2$. The P172C mutant protein of PomA was not functional and inhibits the motility of the wild-type cell in the absence of reducing reagents, although motility was restored by dithiothreitol. These results suggest that a cross-link formed between two molecules of Cys-PomA via $loop_{3-4}$ inhibits the function of the torque-generating units. Residue P172 by itself does not seem to be essential for motor function, since motility is normal in PomA mutants in which P172 was replaced by various amino acids other than Cys. The flexibility of $loop_{3-4}$ seems to be restricted by the cross-linking, thereby impairing motor function. There are at least three possible mechanisms for this inhibition of motor function: (i) Na^+ influx is inhibited by disruption of the channel structure; (ii) conversion of the Na^+ influx to conformational changes in the torque-generating stator units is inhibited; (iii) interactions between the stator and the rotor are inhibited.

The mutant PomA D31C, which is located at the N-terminal periplasmic loop, $loop_{1-2}$, does not swim at low concentrations of Na^+ in the medium, which means that a higher threshold is required for retaining the motility of this mutant [68]. Introduction of positive charges (D31K and D31R) or large structural changes (D31A and D31Y) result in greater shifts of the threshold than in the D31C mutant. On the other hand, replacement by a negatively charged residue (D31E) results in the same dependence on Na^+ as the wild-type PomA. The negative charge of position 31 in PomA probably has an important role for retaining the Na^+ influx through the motor or effective torque generation. It is speculated that the negative charge of Asp^{31} itself or the circumstance of the region including Asp^{31} is possibly involved in the guidance of Na^+ into the channel complex. Direct measurement of the Na^+ current is necessary to clarify the recruitment of ions at the loop region.

6. Recognition of Na^+

Only two kinds of rotary motors, the flagellar motor and the F_1F_o-ATPase, are known in biological systems. Both systems are classified into two types according to the coupling ions, H^+-driven type and Na^+-driven type. F_1F_0-ATPase (also known as ATP synthase) is composed of two parts. The F_1 part is soluble and has ATP synthesis and ATP hydrolysis activity. The F_0 part is embedded in the membrane and transports specific ions. F_0 consists of three kinds of subunits, a, b, and c [69]. It was found that a hybrid enzyme composed of the Na^+-type F_0 part of *Propionigenium modestum* and the H^+-type F_1 part of *E. coli* has Na^+-pumping activity, and H^+-pumping activity is observed only in the absence of Na^+ [70–72]. This suggests that the F_0 part can essentially conduct Na^+ as well as H^+. From mutation analysis it is inferred that an ion specificity site is present in subunits a and c of the F_0 part [73,74].

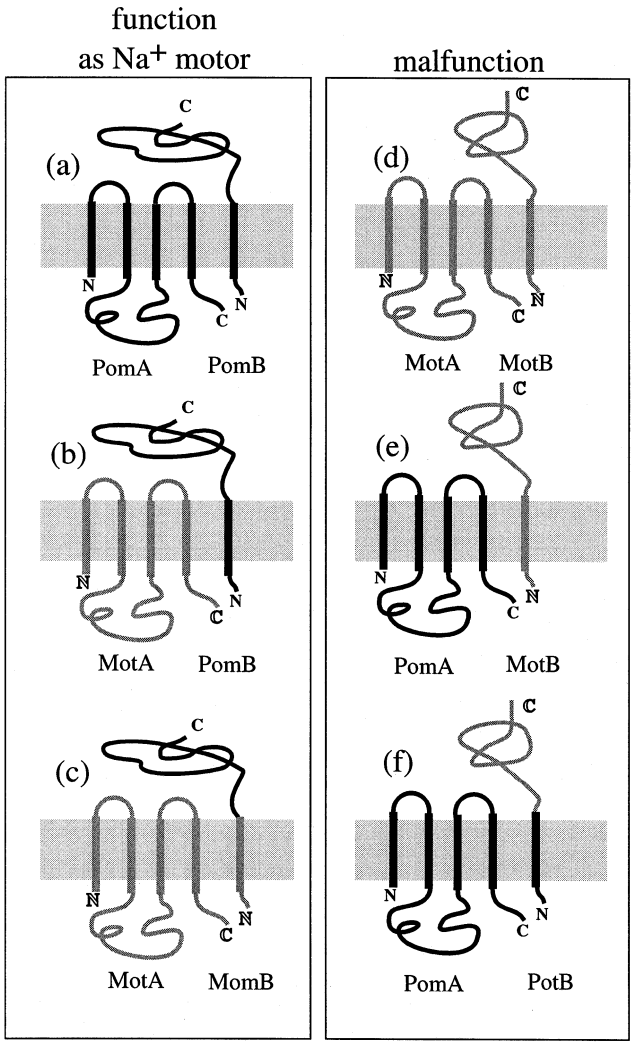

Fig. 6. Hybrid and chimeric motors with the Na^+- and the H^+-driven components. MotA of *R. sphaeroides* or PomA of *V. alginolyticus*, and MotB of *R. sphaeroides* or PomB of *V. alginolyticus* or chimeras between PomB and MotB were expressed in *pom* mutants of *V. alginolyticus*. Black lines and gray lines show the regions of the Na^+- and the H^+-driven component, respectively. The regions of the thick line show the transmembrane regions. The light gray boxes show the inner membrane. In (a), (b), and (c), the motor functions as the Na^+-driven type. On the other hand, the motors of (d), (e), and (f) do not work by Na^+ or H^+. The schematic representations are illustrated from the data in [75,76].

Analysis of the ion specificity of the torque generator has also been carried out in the bacterial flagellar motor (Fig. 6). MotA and MotB of *Rhodobacter sphaeroides* show the largest sequence similarity to PomA and PomB respectively of *V. alginolyticus*, comparing all currently sequenced Mot proteins of H^+ flagellar motors. When the *R. sphaeroides motA* gene is expressed in a *V. alginolyticus pomA* mutant, motility is restored. However, the motility of a *pomB* mutant is not restored by expressing the *motB* gene. The swimming speed of the *pomA* mutant cell with MotA increases with increasing concentration of Na^+ in the medium. The motility is inhibited by the Na^+ channel inhibitors phenamil and amiloride, but not by the H^+ ionophore CCCP. It is concluded that the hybrid motor composed of the H^+-type and Na^+-type components is functional, and MotA of *R. sphaeroides* can generate torque by coupling with the Na^+ flux in place of PomA of *V. alginolyticus* [75]. The chimeric protein (MomB), which has its N-terminal cytoplasmic region and the entire transmembrane segment derived from MotB of *R. sphaeroides*, and the remaining C-terminal periplasmic part from PomB, functions as a Na^+ motor when co-produced with PomA or MotA [76]. These lines of evidence show that the channel part consisting of the transmembrane segments from the A and B subunits does not discriminate the ions Na^+ and H^+.

The ion specificity of the hybrid F_0F_1-ATPase was determined by the F_0 part. The F_1 part is thought to have only mechanical coupling with the F_0 part and the F_1 part should not be expected to alter the ion specificity of the F_0 part. On the other hand, when the channel part of MotA and MotB, whose specificity is H^+, was incorporated into the Na^+ motor, the specificity was changed to Na^+ channel. *E. coli* H^+ motor components MotA and MotB could function in place of the motor proteins of *V. cholerae* though the motility was severely impaired and the hybrid motor seems to be driven by the H^+-motive force [77]. It has been speculated that the other two Na^+ type-specific components, MotX and MotY, are involved in the ion recognition of the motor. The ion recognition systems between the F_0F_1-ATPase and the flagellar motor appear to differ from each other.

In the H^+-driven motor of *E. coli*, MotB, Asp^{32} has a critical role for the motor function and is speculated to convey H^+ [78]. Asp^{32} is the only conserved acidic residue in all presently known sequences of MotB and its homologs. (The corresponding residue in PomB of *V. alginolyticus* is Asp^{24} [49].) When Asp^{32} is substituted with other residues, all mutants fail to be motile, except for the D32E mu-

tant, which has very slow motility. It is known that overexpression of MotA with the N-terminal 60 residues of MotB, which include the putative transmembrane segment, impairs cell growth [15,16,79,80]. When Asp^{32} is substituted with any other amino acid, the growth retardation is no longer observed. The growth defect is interpreted as being due to increased H^+ permeability of the cell membrane. Asp^{32} of MotB is a good candidate for an H^+ binding site. If this is true, the conserved aspartate residue must be a candidate for the binding site of Na^+ in PomB.

7. Composition and structure of the torque generator

The membrane topology of the H^+-driven motor proteins, MotA and MotB, was investigated by Trp-scanning mutagenesis [18,19]. The residues of the transmembrane segments of MotA and MotB were systematically replaced by Trp and the effect on the motor function was examined. Trp has a large size and hydrophobic character, so it is postulated that if Trp substitution faces the lipid, it would be tolerated, but if Trp faces inside the protein complex, it would not be tolerated. The effect on the function seems to imply the effect on the structure. This strategy suggested a hypothetical structure of the MotA/MotB channel complex. The pattern of the effect on MotA is periodic along the four transmembrane segments in the way of α-helices. On the other hand, substitution of MotB is tolerated at positions close to the periplasmic end of the transmembrane segment, but not at positions close to the cytoplasmic end. These results suggest that a single transmembrane segment of MotB is associated with the segments of MotA at a tilt relative to them and its cytoplasmic end is located in the channel complex. In this model, Asp^{32} of MotB, which might be involved in conducting H^+, faces inwards in the complex.

In the case of the Na^+-driven flagellar motor, unlike that of the H^+-driven motor, little information about the structure of the torque generator is known. However, it seems to be clear that PomA and PomB are directly associated together [51]. When the PomA/PomB complex is purified, the subunit ratio of the complex is estimated to be two PomA to one PomB. The predicted size of a complex of two PomA and one PomB molecules is about 90 kDa [81]. However, the PomA/PomB complex obtained by gel filtration assay was found in fractions of higher molecular size than expected (estimated as 175 kDa). When PomA alone is applied to the gel filtration column, it is eluted as a 55-kDa protein, which is likely to correspond to the homodimer complex of PomA as the size expected for monomeric PomA is 27 kDa. Furthermore, a genetically fused dimer of PomA was constructed. It was observed that this tandem PomA dimer is not only stably produced in the *Vibrio* cell but also enables the motor to function. By gel filtration assay, the tandem PomA dimer is also eluted as a 55-kDa protein. These results strongly suggest that native PomA forms a stable homodimer. Moreover, considering the molecular size of the PomA/PomB complex described above, it is speculated that the PomA/PomB complex is composed of four copies of PomA and two copies of PomB. It is the simplest assumption that the complex is a single force-generating unit. From mutation study of the PomA dimer, it is inferred that both halves of the PomA dimer function together to conduct sodium ions, and cooperatively form an ion recognition site [82]. This suggests that the dimer or the multimer is the functional unit of PomA. At present, less structural information is available for the torque generator of the H^+-driven flagellar motor than for the Na^+-driven motor. In order to elucidate the mechanism of the flagellar motor, it is important to obtain more information on the structure of the torque generator.

8. $^{22}Na^+$ conductance of the PomA/B complex

The PomA/PomB protein complex reconstituted into proteoliposomes electrogenically catalyzes $^{22}Na^+$ influx in response to a K^+ diffusion potential [81]. However, PomA only reconstituted into the proteoliposome has no significant Na^+ uptake activity. Catalysis of the Na^+ uptake by the PomA/PomB complex is effectively inhibited in the presence of phenamil, to be at the same level as that of the proteoliposome without the PomA/PomB complex. It is known that the Na^+-driven flagellar motor of *V. alginolyticus* is driven by Li^+ with lower efficiency [83]. The accumulation of $^{22}Na^+$ is prevented by Li^+, indicating that Na^+ and Li^+ compete for a com-

mon binding site of the channel complex. Using this technique, it would be expected that the physiological features of the slow motility and the molecular features of the Na^+ uptake of the torque generator are directly linked and the relationship at the cell level and the molecular level is discussed in more detail.

9. Torque generation

It is thought that three components, MotA, MotB, and FliG, are directly involved in the torque generation of the H^+-driven flagellar motor (Fig. 7). FliG is a soluble protein and one of the components in the rotor [20,84,85]. Mutational analysis provided identification of the important and conserved residues for the torque generation of MotA and FliG and led to the proposal of a model for the interaction between MotA and FliG (Fig. 7) [21–24]. In this model, it is suggested that three residues, Arg^{281}, Asp^{288} and Asp^{289}, in the C-terminal α-helix of FliG and two residues, Arg^{90} and Glu^{98}, in the cytoplasmic loop region of MotA are important for function. Double mutants with substitution of charged residues synergistically inhibited the motor function. So, it is hypothesized that electrostatic interactions essential for the rotation of the motor occur between the rotor component FliG and the stator component MotA via these residues. The two functionally important residues of MotA are also conserved in PomA of *V. alginolyticus* and the PomA homolog of *V. parahaemolyticus* [49,52]. Recently, the Na^+-driven switch genes including *fliG* have been isolated from *V. parahaemolyticus* and the functionally important charged residues are all conserved in FliG of *V. parahaemolyticus* [86]. It was shown that the rotation of *V. cholerae* flagella is powered by the Na^+ influx [35,36]. There is an open reading frame with a sequence similar to FliG in the genome of *V. cholerae* (from the unfinished genome database) and this open reading frame also conserves those charged residues. This seems to suggest that the rotor component and the stator component electrostatically interact in the Na^+-driven flagellar motor to generate the rotary power as proposed in the H^+-driven flagellar motor. This is supported by the suggestion that MotA of *R. sphaeroides* works with FliG of *V. alginolyticus*, using the energy of Na^+, in *pomA*-defective *Vibrio* cells expressing *motA* [75,76].

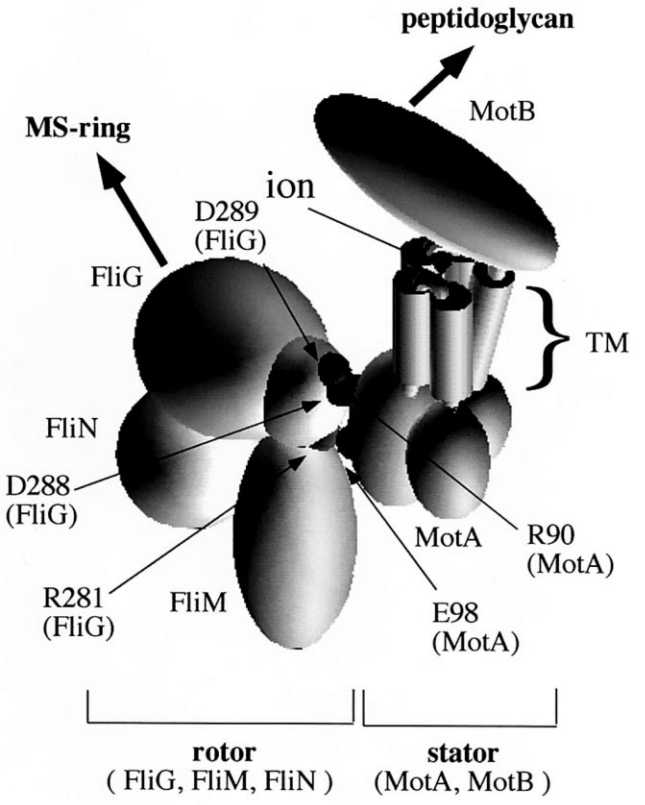

Fig. 7. Rotor and stator in the flagellar motor. A model of a stator unit, which consists of MotA and MotB, and a rotor unit, which consists of FliG, FliM, and FliN, is presented on the assumption that each unit is composed of a single molecule of each component though it may not be true. The rotor units are attached to the MS ring and form a ring structure, the C ring. The C-terminal region of MotB interacts with peptidoglycan to anchor the stator to the cell wall. The charged residues on the rotor–stator interface, which seem to be important for force generation, are indicated by the residue number with an arrow. TM: transmembrane region. The model of this H^+-driven motor should be similar to that of the Na^+-driven motor because the components are exchangeable between the both motors [75–77].

10. Summary

There are four transmembrane components, PomA, PomB, MotX and MotY, required for rotating the Na^+-driven flagellar motor. From the analysis of MotA and MotB in the H^+-driven flagellar motor, PomA and PomB are likely to contact the

rotor component directly and participate in torque generation. However, the function of the two Na^+ type-specific components, MotX and MotY, is unknown though they may be involved in the ion recognition of the motor. How are these components involved in the generation of the torque? To understand the functional role of MotX and MotY it is important to understand the mechanism of the coupling between Na^+ influx and rotary power, since these proteins are specifically found in the Na^+-driven flagellar motor. Comparatively easy manipulation of Na^+ will be greatly advantageous for the study of MotX and MotY.

Two rotary motors are known in live organisms, one is the bacterial flagellar motor and the other is F_1F_0-ATPase. The latter motor has been well studied and detailed models of the rotary mechanism have been advanced. We believe that resolving the crystal structure is an important contribution to the developing study of the F_1F_0-ATPase. For not only the Na^+- but also the H^+-driven flagellar motor, more structural knowledge of the torque generator is required for understanding the rotary mechanism.

Acknowledgements

We thank Drs. Richard M. Berry, Ikuro Kawagishi, and Toshiharu Yakushi for critically reading the manuscript. The work in our laboratory was supported in part by Grants-in-Aid for Scientific Research from the Ministry of Education, Science and Culture of Japan. T.Y. was supported by the Japan Society for the Promotion of Science.

References

[1] S. Khan, J. Bacteriol. 175 (1993) 2169–2174.
[2] D.F. Blair, Annu. Rev. Microbiol. 49 (1995) 489–522.
[3] R.M. Macnab, in: Neidhardt et al. (Eds.), *Escherichia coli* and *Salmonella typhimurium*: Cellular and Molecular Biology, 2nd edn., American Society for Microbiology, Washington, DC, 1996, pp. 123–145.
[4] D.J. DeRosier, Cell 93 (1998) 17–20.
[5] M.D. Manson, P. Tedesco, H.C. Berg, F.M. Harold, C. van der Drift, Proc. Natl. Acad. Sci. USA 74 (1977) 3060–3064.
[6] S. Matsuura, J. Shioi, Y. Imae, FEBS Lett. 82 (1977) 187–190.
[7] S.H. Larsen, J. Adler, J.J. Gargus, R.W. Hogg, Proc. Natl. Acad. Sci. USA 71 (1974) 1239–1243.
[8] A.N. Glagolev, V.P. Skulachev, Nature 272 (1978) 280–282.
[9] G.D. Dean, R.M. Macnab, J. Stader, P. Matsumura, C. Burks, J. Bacteriol. 159 (1984) 991–999.
[10] J. Stader, P. Matsumura, D. Vacante, G.E. Dean, R.M. Macnab, J. Bacteriol. 166 (1986) 244–252.
[11] J.D. Zhou, R.T. Fazzio, D.F. Blair, J. Mol. Biol. 251 (1995) 237–242.
[12] S.Y. Chun, J.S. Parkinson, Science 239 (1988) 276–278.
[13] R. De Mot, J. Vanderleyden, Mol. Microbiol. 12 (1994) 333–334.
[14] R. Koebnik, Mol. Microbiol. 16 (1995) 1269–1270.
[15] D.F. Blair, H.C. Berg, Cell 60 (1990) 439–449.
[16] B. Stolz, H.C. Berg, J. Bacteriol. 173 (1991) 7033–7037.
[17] A.G. Garza, L.W. Harrishaller, R.A. Stoebner, M.D. Manson, Proc. Natl. Acad. Sci. USA 92 (1995) 1970–1974.
[18] L.L. Sharp, J.D. Zhou, D.F. Blair, Proc. Natl. Acad. Sci. USA 92 (1995) 7946–7950.
[19] L.L. Sharp, J.D. Zhou, D.F. Blair, Biochemistry 34 (1995) 9166–9171.
[20] S.A. Lloyd, H. Tang, X. Wang, S. Billings, D.F. Blair, J. Bacteriol. 178 (1996) 223–231.
[21] S.A. Lloyd, D.F. Blair, J. Mol. Biol. 266 (1997) 733–744.
[22] J. Zhou, D.F. Blair, J. Mol. Biol. 273 (1997) 428–439.
[23] J. Zhou, S.A. Lloyd, D.F. Blair, Proc. Natl. Acad. Sci. USA 95 (1998) 6436–6441.
[24] S.A. Lloyd, F.G. Whitby, D.F. Blair, C.P. Hill, Nature 400 (1999) 472–475.
[25] Y. Imae, T. Atsumi, J. Bioenerg. Biomembr. 21 (1989) 705–716.
[26] K. Ota, A. Kiyomiya, N. Koyama, Y. Nosoh, J. Gen. Microbiol. 86 (1975) 259–266.
[27] T.A. Krulwich, M. Ito, R. Gilmour, M.G. Sturr, A.A. Guffanti, D.B. Hicks, Biochim. Biophys. Acta 1275 (1996) 21–26.
[28] N. Hirata, M. Kitada, Y. Imae, FEBS Lett. 132 (1981) 278–280.
[29] N. Hirata, Y. Imae, J. Biol. Chem. 258 (1983) 10577–10580.
[30] S. Sugiyama, H. Matsukura, Y. Imae, FEBS Lett. 182 (1985) 265–268.
[31] Y. Imae, H. Matsukura, S. Kobayasi, Methods Enzymol. 125 (1986) 582–592.
[32] B.V. Chernyak, P.A. Dibrov, A.N. Glagolev, M.Y. Sherman, V.P. Skulachev, FEBS Lett. 164 (1983) 38–42.
[33] P.A. Dibrov, V.A. Kostyrko, R.L. Lazarova, V.P. Skulachev, I.A. Smirnova, Biochim. Biophys. Acta 850 (1986) 449–457.
[34] T. Atsumi, L.L. McCarter, Y. Imae, Nature 355 (1992) 182–184.
[35] C.C. Hase, J.J. Mekalanos, Proc. Natl. Acad. Sci. USA 96 (1999) 3183–3187.
[36] S. Kojima, K. Yamamoto, I. Kawagishi, M. Homma, J. Bacteriol. 181 (1999) 1927–1930.
[37] I. Kawagishi, Y. Maekawa, T. Atsumi, M. Homma, Y. Imae, J. Bacteriol. 177 (1995) 5158–5160.

[38] L.L. McCarter, M. Hilmen, M. Silverman, Cell 54 (1988) 345–351.
[39] L.L. McCarter, M. Silverman, Mol. Microbiol. 4 (1990) 1057–1062.
[40] T. Atsumi, Y. Maekawa, T. Yamada, I. Kawagishi, Y. Imae, M. Homma, J. Bacteriol. 178 (1996) 5024–5026.
[41] H. Tokuda, J. Bioenerg. Biomembr. 20 (1989) 693–704.
[42] H. Tokuda, M. Asano, Y. Shimamura, T. Unemoto, S. Sugiyama, Y. Imae, J. Biochem. 103 (1988) 650–655.
[43] L.L. McCarter, J. Bacteriol. 176 (1994) 4219–4225.
[44] L.L. McCarter, J. Bacteriol. 176 (1994) 5988–5998.
[45] I. Okunishi, I. Kawagishi, M. Homma, J. Bacteriol. 178 (1996) 2409–2415.
[46] M. Furuno, N. Nishioka, I. Kawagishi, M. Homma, Microbiol. Immunol. 43 (1999) 39–43.
[47] S. Sugiyama, E.J. Cragoe Jr., Y. Imae, J. Biol. Chem. 263 (1988) 8215–8219.
[48] M.L. Wilson, R.M. Macnab, J. Bacteriol. 172 (1990) 3932–3939.
[49] Y. Asai, S. Kojima, H. Kato, N. Nishioka, I. Kawagishi, M. Homma, J. Bacteriol. 179 (1997) 5104–5110.
[50] S. Kojima, M. Kuroda, I. Kawagishi, M. Homma, Microbiology 145 (1999) 1759–1767.
[51] T. Yorimitsu, K. Sato, Y. Asai, I. Kawagishi, M. Homma, J. Bacteriol. 181 (1999) 5103–5106.
[52] S. Jaques, Y.K. Kim, L.L. McCarter, Proc. Natl. Acad. Sci. USA 96 (1999) 5740–5745.
[53] S. Kudo, Y. Magariyama, S.-I. Aizawa, Nature 346 (1990) 677–680.
[54] K. Muramoto, I. Kawagishi, S. Kudo, Y. Magariyama, Y. Imae, M. Homma, J. Mol. Biol. 251 (1995) 50–58.
[55] Y. Magariyama, S. Sugiyama, K. Muramoto, I. Kawagishi, Y. Imae, S. Kudo, Biophys. J. 69 (1995) 2154–2162.
[56] Y. Magariyama, S. Sugiyama, K. Muramoto, Y. Maekawa, I. Kawagishi, Y. Imae, S. Kudo, Nature 381 (1994) 752.
[57] G. Lowe, M. Meister, H.C. Berg, Nature 325 (1987) 637–640.
[58] R.M. Berry, J.P. Armitage, Adv. Microb. Physiol. 41 (1999) 291–337.
[59] E.J. Cragoe Jr., T.R. Kleyman, L. Simchowitz, Amiloride and Its Analogs: Unique Cation Transport Inhibitors, VCH, New York, 1992.
[60] K. Muramoto, S. Sugiyama, E.J. Cragoe Jr., Y. Imae, J. Biol. Chem. 269 (1994) 3374–3380.
[61] S.M. Block, H.C. Berg, Nature 309 (1984) 470–472.
[62] D.F. Blair, H.C. Berg, Science 242 (1988) 1678–1681.
[63] S. Khan, M. Dapice, T.S. Reese, J. Mol. Biol. 202 (1988) 575–584.
[64] S. Kojima, T. Atsumi, K. Muramoto, S. Kudo, I. Kawagishi, M. Homma, J. Mol. Biol. 265 (1997) 310–318.
[65] S. Kojima, Y. Asai, T. Atsumi, I. Kawagishi, M. Homma, J. Mol. Biol. 285 (1999) 1537–1547.
[66] Y. Asai, T. Shoji, I. Kawagishi, M. Homma, J. Bacteriol. 182 (2000) 1001–1007.
[67] T. Yorimitsu, K. Sato, Y. Asai, M. Homma, J. Biol. Chem. 275 (2000) 31387–31391.
[68] S. Kojima, T. Shoji, Y. Asai, I. Kawagishi, M. Homma, J. Bacteriol. 182 (2000) 3314–3318.
[69] R.H. Fillingame, in: T.A. Krulwich (Ed.), Molecular Mechanics of ATP Synthesis by F_1F_0-type H^+-Translocating ATP Synthases: The Bacteria, Vol. 12, Academic Press, New York, 1990, pp. 345–391.
[70] W. Laubinger, H.G. Deckers, K. Altendorf, P. Dimroth, Biochemistry 29 (1990) 5458–5463.
[71] G. Kaim, P. Dimroth, Eur. J. Biochem. 218 (1993) 937–944.
[72] G. Kaim, P. Dimroth, Eur. J. Biochem. 222 (1994) 615–623.
[73] Y. Zhang, R.H. Fillingame, J. Biol. Chem. 270 (1995) 87–93.
[74] G. Kaim, P. Dimroth, Biochemistry 37 (1998) 4626–4634.
[75] Y. Asai, I. Kawagishi, R.E. Sockett, M. Homma, J. Bacteriol. 181 (1999) 6322–6328.
[76] Y. Asai, I. Kawagishi, R.E. Sockett, M. Homma, EMBO J. 19 (2000) 3639–3648.
[77] K.K. Gosink, C.C. Hase, J. Bacteriol. 182 (2000) 4234–4240.
[78] J. Zhou, L.L. Sharp, H.L. Tang, S.A. Lloyd, S. Billings, T.F. Braun, D.F. Blair, J. Bacteriol. 180 (1998) 2729–2735.
[79] M.L. Wilson, R.M. Macnab, J. Bacteriol. 170 (1988) 588–597.
[80] D.F. Blair, H.C. Berg, J. Mol. Biol. 221 (1991) 1433–1442.
[81] K. Sato, M. Homma, J. Biol. Chem. 275 (2000) 5718–5722.
[82] K. Sato, M. Homma, J. Biol. Chem. 275 (2000) 20223–20228.
[83] J.Z. Liu, M. Dapice, S. Khan, J. Bacteriol. 172 (1990) 5236–5244.
[84] S. Yamaguchi, S. Aizawa, M. Kihara, M. Isomura, C.J. Jones, R.M. Macnab, J. Bacteriol. 168 (1986) 1172–1179.
[85] V.M. Irikura, M. Kihara, S. Yamaguchi, H. Sockett, R.M. Macnab, J. Bacteriol. 175 (1993) 802–810.
[86] B.R. Boles, L.L. McCarter, J. Bacteriol. 182 (2000) 1035–1045.